Computational Materials Science 170 (2019) 109190

Contents lists available at ScienceDirect

Computational Materials Science

journal homepage: www.elsevier.com/locate/commatsci

Reveal the fast and charge-insensitive lattice diffusion of silver in cubic silicon carbide via first-principles calculations

Qing Peng[a,b,*], Nanjun Chen[a], Zhijie Jiao[a], Isabella J. van Rooyen[c], William F. Skerjanc[d], Fei Gao[a,*]

[a] Nuclear Engineering and Radiological Sciences, University of Michigan, Ann Arbor, MI 48109, USA
[b] Department of Mechanical, Aerospace and Nuclear Engineering, Rensselaer Polytechnic Institute, Troy, NY 12180, USA
[c] Fuel Design and Development Department, Idaho National Laboratory, Idaho Falls, ID 83415-6188, USA
[d] Reactor Physics Design and Analysis Department, Idaho National Laboratory, Idaho Falls, ID 83415-6188, USA

ARTICLE INFO

Keywords:
Silicon carbide
Lattice diffusion
First-principles calculations
Radiation damage
Silver release

ABSTRACT

The lattice diffusion of silver with various charge states in cubic silicon carbide has been investigated by means of high-fidelity spin-polarized density functional theory calculations. The migration energy barrier of the Ag interstitial diffusion is 1.09 eV and 1.11 eV for neutral and $q = +1e$ charge state, respectively, close to the activation energy of Ag diffusion measured in the German HTR fuel program. A general trend is that the migration energy barrier reduces with respect to the increase of charge on Ag, which is much less than the increment in the oxidation energy, suggesting that the lattice diffusion of silver prefers constant neutral state without redox in transition state. Our results indicate a scenario that once Ag is deposited to interstitials via the kickout mechanism, it will highly likely perform lattice diffusion across the SiC layer leading to fast release of Ag in Tristructural-Isotropic fuel induced by irradiation.

1. Introduction

As one of the most important compound semiconductors, silicon carbide (SiC) has shown exceptional properties such as wide bandgap, high hardness and Young's modulus, high thermal conductivity (better than Cu), good thermal shock resistance, low thermal expansion and good chemical inertness [1]. SiC is widely used in nuclear engineering as structural materials and micro-electronics as semiconductors. Silver (Ag) is an important interconnect material for power electronics packaging, with advantages of high thermal and electrical conductivities, and lead-free composition [2]. The lattice diffusion of silver might cause the current leakage, aging and degradation of the materials, and malfunction of the micro-electronics. Besides electronics, SiC is also a stiff structural material. Due to its ultra-high stiffness, SiC is a key component material in Tristructural-Isotropic (TRISO)-coated fuel, which is a type of micro-fuel particle that is to be used in the next generation of Very High Temperature Reactors [3]. TRISO fuel is designed to contain fission products, the main sources of radiation, within the coated particle fuels using silicon carbide as a diffusion barrier [4]. Therefore, the knowledge of the diffusion behaviors of fission products in SiC is the key to design TRISO and retain the high temperature gas-cooled reactors functionality which have advantages over conventional reactors including high efficiency and safety. The silicon carbide layer has received particular attention because it is considered to be a primary diffusion barrier against the diffusion of fission products from the fuel to the reactor coolant, in addition to the structural stability and integrity of TRISO. Studies have shown that silver $^{110}{}_m$Ag can apparently diffuse through silicon carbide and be released through intact SiC [5–8,7,9,10]. $^{110}{}_m$Ag is a highly radioactive isotope with half-life of 253 days, produced by neutron captivation by ^{109}Ag, a stable isotope of low fission yield, of which only 0.1% is converted. Because $^{110}{}_m$Ag is a strong γ-ray emitter, this unprecedented release raises potential safety concerns of TRISO during maintenance activities, and contributes to restriction on higher operating temperature and associated increased fuel efficiency of the new generation of reactors [11].

Extensive studies have aimed to address this problem of $^{110}{}_m$Ag release without convincing conclusions. For convenience, the $^{110}{}_m$Ag will further be referred to as just Ag unless specified. Some authors have attributed this phenomenon to the presence of excess silicon [6], chemical degradation of SiC [12,9], nanopores, [8,10,13], the existence of long columnar grains, formation of nanocracks [6,10,14], grain boundaries [15,16,7,17–20], nodule transport assisted by Palladium [21,22], and reaction-wetting process [23]. Shrader et. al. investigated the Ag diffusion in cubic silicon carbide using Density Functional

* Corresponding authors at: Nuclear Engineering and Radiological Sciences, University of Michigan, Ann Arbor, MI 48109, USA (Q. Peng and F. Gao).
E-mail addresses: qpeng.org@gmail.com (Q. Peng), gaofeium@umich.edu (F. Gao).

https://doi.org/10.1016/j.commatsci.2019.109190
Received 9 June 2019; Received in revised form 5 August 2019; Accepted 5 August 2019

Theory (DFT) calculations [24]. They reported that the impurity state with the lowest activation energy for lattice diffusion is found to be the Ag interstitial, with an effective activation energy of 7.88 eV. They concluded that the Ag lattice diffusion is very slow and is not able to account for the relatively fast diffusion seen in integral release measurements on poly-crystalline SiC. Numerical theoretical studies then focus on the diffusion of Ag along the grain boundaries [25–27,11], or surface diffusion [14]. However, long-term annealing studies of ion implanted silver in SiC showed no evidence for silver migration along grain boundaries [23]. A recent study [28] contradict the grain boundary diffusion mechanism for Ag release from SiC fabricated by fluidized-bed chemical vapor deposition (FBCVD) as the long held assumption. Post irradiation tests of UCO kerneled TRISO coated particles from the US advanced gas reactor experiments provided more insight on fission product distributions through advanced electron microscopy and micro-analytical work. These examinations revealed the strong presence of Ag, amongst other fission products, at grain boundaries with precipitates of Ag in only two cases of over 700 areas studied [29–32]. Several recent experimental investigations do not support the grain boundary diffusion mechanism [33,34]. Additionally, van Rooyen et al. [35] hypothesized that the Ag-transport mechanism is likely more complex and may be a combination of several mechanisms.

The lattice diffusion of Ag is critical in discovering the diffusion mechanism in 3C-SiC, because it always serves as a starting point and reference for discussion of other mechanisms, including grain boundary, nanocracks, nanopores, and surface mechanisms. The lattice diffusion would dominate the diffusion process at the large grain sizes and high temperatures (> 1600 °C) [36]. In addition, the influence of the charge status to the migration energy barrier of Ag is still unknown. Therefore, it is necessary to revisit this important issue and set a rigid and reliable reference for any further exploration of the silver release.

The goal of this paper is to re-assess the lattice diffusion of Ag in 3C-SiC single crystal. We focus on the Ag interstitial diffusion mechanism since it has been shown that intrinsic diffusion of the Ag interstitials is faster than substitutional diffusion [24]. We carried out high accurate spin-polarized DFT calculations at GGA-PBEsol level in a large simulation cell (217 atoms) to ensure the accuracy is within 0.02 eV/cell. As a prior effort, we have investigated the formation energies of the formation energies of point defects including Ag interstitials [37]. In this study, the diffusion path of the Ag interstitial diffusion was firstly investigated. Then we studied the minimum energy pathways of the Ag diffusion with different charge states. We found a substantial (about 0.19 eV) higher diffusion barrier than previous reported. Our results of the Ag lattice diffusion barriers might serve a new standard and solid ground in searching for the mechanisms and solutions of the unprecedented Ag release in TRISO fuel.

The remainder of the paper is organized as follows. Section 2 presents the computational method, including the computational details of DFT calculations and the Nudged Elastic Band (NEB) calculations. The results and analysis are in Section 3, followed by conclusions in Section 4.

2. Density functional theory calculations

The conventional unit cell contains eight atoms (four silicon and four carbon atoms). A single Ag atom has a relatively large atom radius of 2.11 Å, referring to that of carbon atom (0.74 Å) and Si atoms (1.14 Å). To reduce the artificial interactions between images and their long range elastic fields induced by interstitial Ag, we used a $3 \times 3 \times 3$ super-cell containing 217 atoms, which consists of 108 silicon and 108 carbon atoms with one silver atom as an interstitial. Our previous efforts illustrate that such a configuration is sufficient for point defect investigation [37].

The total energies of the system and forces on each atoms are characterized via first-principles calculations within the framework of DFT. All DFT calculations were carried out with the Vienna Ab-initio Simulation Package (VASP) [38,39] which is based on the Kohn-Sham Density Functional Theory (KS-DFT) [40,41] with the generalized gradient approximations of the exchange-correlation functions [42] as parameterized by Perdew, Burke and Ernzerhof (PBE) revised for solids (PBEsol) [43]. The electrons explicitly included in the calculations are the $2s^2 2p^2$, $3s^2 3p^2$, $5s^1 4d^{10}$ electrons for carbon, silicon, and silver atoms, respectively. The core electrons are replaced by the projector augmented wave (PAW) and pseudo-potential approach [44,45]. A plane-wave cutoff of 520 eV is used in the geometry relaxation to reduce Pulay stress. For all other calculations, we used a plane-wave cutoff of 400 eV with accurate and dense *k*-mesh. The irreducible Brillouin Zone was sampled with a Gamma-centered $3 \times 3 \times 3$*k*-mesh for all the calculations. The calculations are performed at zero temperature. The criterion to stop the relaxation of the electronic degrees of freedom is set by total energy change to be smaller than 10^{-5} eV. The optimized atomic geometry was achieved through minimizing Hellmann-Feynman forces acting on each atom until the maximum forces on the ions were smaller than 0.01 eV/Å.

The Ag interstitial formation energy are computed using a super-cell formalism with Freysoldt, Neugebauer and Van de Walle (FNV) scheme [46]. In general, for a defect or impurity X in a charge state q, its formation energy $E^f(X^q)$ is computed by [47]

$$E^f(X^q, E_F) = E^{tot}(X^q) - E^{tot}_{bulk}(q = 0) - \sum_i \Delta n_i \nu_i + q(E_{VBM} + E_F) + E^{corr}, \quad (1)$$

where $E^{tot}(X^q)$ is the total energy of the super-cell containing the defect X in the charge state q, $E^{tot}_{bulk}(q = 0)$ denotes the total energy of the pristine bulk super-cell which is neutral and free of any defects, Δn_i represents the number of atoms of species i added to ($\Delta n_i > 0$) or removed from ($\Delta n_i < 0$) the super-cell as a result of the defect formation, and ν_i corresponds to the chemical potential of element species i. When a silver atom is added to the system, the associated electrons are also added to the system and contribute to the formation energy. Such a contribution is described by the chemical potential of electrons, known as the Fermi level E_F at zero temperature. Here, E_F of a semiconductor is treated as an independent variable that can take any value within the bandgap. It is worth noting that E_F is measured with respect to E_{VBM}, the energy of valence band maximum (VBM) of the bulk material. The correction term E^{corr} counts the image charge interaction and the potential alignment between the perfect and defected structures as formulated by FNV scheme [46].

We used the climbing image nudged elastic band (CI-NEB) method [48] to compute the diffusion pathways and the corresponding minimum energy path. To calculate the migration energy barrier, we first do a full relaxation of the initial configuration so that all degrees of freedoms, both the lattice atoms and the lattice vectors are allowed to move during the relaxation. After the geometry relaxation, the residue stresses within the simulation box are small, less than 0.1 GPa. Then we only relax the atoms' positions of T_{Si} (tetrahedral position surrounded by four Si atoms) configurations while keeping the lattice vector the same as that of the relaxed T_C (tetrahedral position surrounded by four C atoms) configurations. After the geometry relaxation of the both initial and final configurations, we perform CI-NEB calculations. Typically, 10 images, including initial and final states, were used in the CI-NEB calculations for accurate modeling.

3. Results and analysis

3.1. Atomic structure

The single crystalline 3C-SiC has a cubic crystal structure (Zinc Blende) with space group number of 216 and group symmetry $T_d^2 - F43m$. Our results of the lattice constants is $a = 4.38$ Å, agreeing excellently with experimental data ($a = 4.36$ Å) [49] and previous DFT

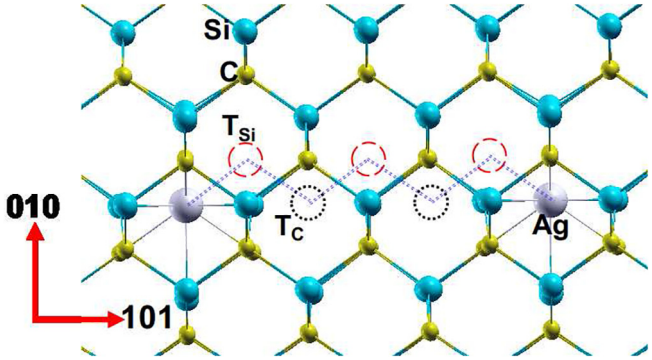

Fig. 1. Geometry and diffusion path. The 3C-SiC lattice and the geometry of the minimum energy pathways of the Ag diffusion in the bulk 3C-SiC via interstitials along a "zigzag" path of T_C-T_{Si}-T_C. The small yell ball denotes carbon atoms, medium water-blue balls denotes Si atoms, large silver balls denotes Ag atoms; dotted (dashed) circles denotes the possible T_C (T_{Si}) site.

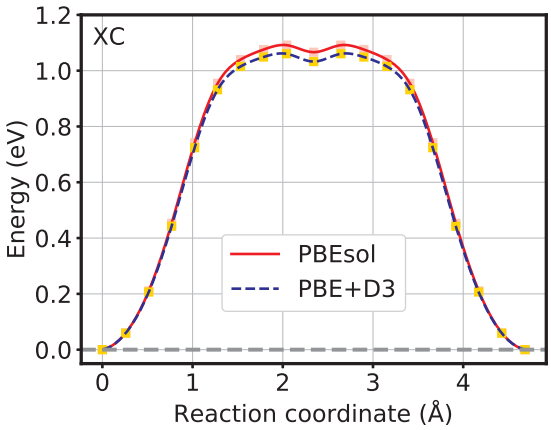

Fig. 2. Exchange-Correlation functional effect. The minimum energy pathways of the Ag diffusion in the bulk 3C-SiC along the pathways from a 4-Carbon atoms formed tetrahedron site (T_C) to the nearest T_C site through the nearest 4-Silicon atoms formed tetrahedron site (T_{Si}), predicted using different exchange correlation functionals.

calculation of $a = 4.37$ Å[50]. The bond length of C-Si bond is 1.888 Å.

Besides the PBEsol exchange-correlation functions, we have tested the PBE-D3 calculations [51], which give the lattice constant of 4.38 Å, and atomic volume of 10.50 Å^3, agreeing well with the PBEsol results. The vdW-DFq study [52] also gives similar results.

When a silver atom becomes an interstitial in the 3C-SiC crystal lattice, there are quite a few possible positions that the silver atom can be allocated. Our previous study shows that the two positions of tetrahedron sites, namely T_C and T_{Si} have the two lowest formation energies of interstitials, which is 8.70 and 9.80 eV, respectively. These two positions are depicted in the Fig. 1. Therefore, the possible lattice diffusion paths of the interstitial silver are along these tetrahedron sites. Among them, the diffusion path along the successive T_C-T_{Si}-T_C is the most possible lattice diffusion path. To have a better view of this T_C-T_{Si}-T_C diffusion path, we rotate the coordinate system so that the x and y axis is along the [1 0 1] and [0 1 0] direction, respectively, as shown in Fig. 1. We only denote the diffusion along the x axis here for convenience, the diffusion path of this T_C-T_{Si}-T_C is three-dimensional, and the trace does not need to be straight line. The diffusion paths are a collection of all possible segments along ⟨1 0 1⟩ directions.

This investigation focus on the migration energy barrier of the lattice diffusion of Ag along the diffusion path of T_C-T_{Si}-T_C, because it is the most possible and fastest diffusion path of an interstitial Ag atom. We have considered the diffusion of a neutral Ag atom first, followed by the influence of the charge states on the diffusion.

3.2. Migration energy barrier of a neutral Ag atom

The minimum energy pathways of a neutral Ag diffusion in the bulk 3C-SiC along the pathways of T_C-T_{Si}-T_C are shown in Fig. 2. The diffusion is the hop segments along ⟨1 0 1⟩ directions. The length of each segment is 2.33 Å. The initial state (reaction coordinate at 0 Å) is the configuration that a neutral Ag atom in the T_C site. The whole minimum energy pathway of T_C-T_{Si}-T_C has two segments T_C-T_{Si} and T_{Si}-T_C which are individually obtained through the Climbing-Image nudged elastic band method.

The middle state (the reaction coordinate at 2.33 Å) is the configuration that the neutral Ag atom in the T_{Si} site that is the nearest tetrahedra (T) site neighbor to the initial state. The middle state T_{Si} has a higher potential energy (1.066 eV) than the initial state of T_C. The final state (the reaction coordination at 4.66 Å) is the T_C site that is the nearest T site neighbor to the middle state. The potential energy at the initial state is set to 0. Then the migration energy barrier is 1.0819 eV, and the middle state energy is 1.066 eV. The whole system is neutral with zero net charge.

We also examined the influence of the exchange-correlation functionals on the calculations of the migration energy barriers for sake of our quantitative investigations. Our results from PBE-D3 calculations are 1.061 and 1.033 eV for the migration energy barrier and the T_{Si} site potential energy, respectively, which agrees well with the PBEsol calculations, as illustrated in Fig. 2. The largest difference is only 0.033 eV, which could be regarded as the precision of the migration energy barrier in this investigation.

Our result of the migration energy barrier of 1.082 eV for the neutral Ag interstitial lattice diffusion is 0.192 eV higher than previous DFT investigations [24], which used a relatively smaller super-cell ($2 \times 2 \times 2$) with 64 + 1 atoms. Our results suggest that the smaller super-cell of ($2 \times 2 \times 2$) is not capable to predict the migration energy barrier of lattice diffusion of Ag in 3C-SiC, and a larger super-cell at least ($3 \times 3 \times 3$) is required for quantitative investigation. In addition, we have explicitly included non-local van der Waals interactions in DFT calculations which were missing in the previous studies. Our more accurate results set a rigorous ground and reference for further investigation of the other diffusion mechanisms of Ag release in TRISO fuel.

3.3. Charge effect

The charge status of Ag during the lattice diffusion in 3C-SiC is still an open question. To shed a light on this issue, we study the diffusion behaviors with different charge status. Explicitly, we investigate the 5 different charge states ranged from 0 to +4 for Ag atoms/ions. The negatively charged states are not considered because they are unlikely to happen, as the formation energy becomes larger with the negative charges.

The minimum energy pathways of the charged Ag ions diffusion in the bulk 3C-SiC along the pathways of T_C-T_{Si}-T_C are depicted in Fig. 3, compared with that of the neutral Ag atoms. We have examined the system with spin-polarized DFT calculations in addition to the classical non spin-polarized DFT calculations. The magnetic moments of all the configurations of Ag interstitial in this study are zero, including their transition states. The charge state has no effect on the magnetic moments. Our results show that the charge state of Ag affects the minimum energy pathway profiles. It is of great interest to note that both the diffusion energy barriers and the positions of the barriers are influenced by the charge state. The energy barriers, however, are less prone to the charge states. The maximum diffusion barrier energy of 1.11 eV is presented when Ag has $+1e$ charge.

For convenience, we list the migration energy barrier data in the Table 1, along with the relative formation energy of the interstitials T_{Si}

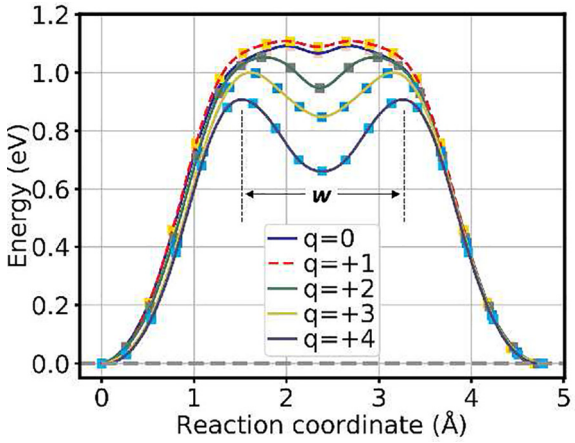

Fig. 3. Charge effect. The minimum energy pathways of the interstitial Ag diffusion with 5 different charge states ranged from 0 to +4*e*. The reference energy of each charge state is that of Ag interstitial at T_C site with the same charge state.

Table 1
Charge influence. The influence of charge state on the migration energy barriers E_a, relative formation energy E^f of T_{Si} configurations, and the potential width of the local minimum of T_{Si} configurations w shown in Fig. 3.

	E_a (eV)	E^f (eV)	w (Å)
q = 0	1.092	1.066	0.667
q = +1e	1.107	1.089	0.834
q = +2e	1.053	0.947	1.421
q = +3e	0.998	0.848	1.746
q = +4e	0.894	0.661	1.847

to T_C , and the width w of the local minimum of the T_{Si} configurations in the minimum energy pathway profiles illustrated in Fig. 3. This parameter w quantify the migration path profile by measuring the width between the local minimums along the diffusion path. Accompanied with the depth of the local minimum, it could be useful to obtain the vibration frequencies during the diffusion. The detailed discussion and the comparison with the experiments are presented in the following subsections.

Besides the diffusion energy barrier, the prominent difference is the relative formation energy of the T_{Si} configuration in the minimum energy pathway profiles for different charge states. The relative formation energy (E^f) is defined as the energy difference between the two tetrahedron interstitial configurations T_{Si} and T_C, as $E^f(q) = E^f(T_{Si}(q)) - E^f(T_C(q))$. The variation of the E^f with respect to the charge state is summarized in Table 1. The neutral state is corresponding to $E^f = 1.0666$ eV. The maximum value of 1.13 eV appears at the charge state of +1e. Beyond that E^f decreases with an increment of the charge. This is quite reasonable because in general the formation energy of a defect in a semiconductor dependents on the Fermi energy of the system which depends on many factors including introduction of defects and charges [24]. Despite these variations, the diffusion energy barrier is quite similar. The diffusion energy barriers are insensitive to the charge state of the Ag in lattice diffusion via interstitials.

Furthermore, we observed that the width of the potential well w around the local minimum of T_{Si} configuration varies with the charge state in the minimum energy pathway profiles. The width of the potential well as a function of the charge state is listed in Table 1. The w monotonically increases with respect to an increase of charge. When the charge reaches +4e, the w shows a saturation which is only 0.01 Å increment. Our results shows that the over charged Ag ions are more stable in the 3C-SiC.

It is worth noting that we have checked the charge localization and

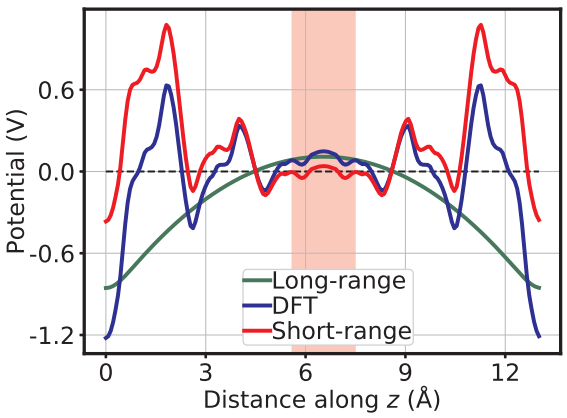

Fig. 4. Charge localization and potential alignment. Planar averaged potential alignment correction on Ag interstitial in cubic SiC with charge state of q = +4e using FNV scheme[46]. The defect Ag is located at the center of a 3 × 3 × 3 cubic SiC super-cell. The green curve is the model point charge for long-range correction. The pink region is the sampling region for obtaining the potential alignment correction, according to Ref. [46].

potential alignment using FNV scheme [46]. The defect Ag is shifted to the origin (0,0,0) of the super-cell. The potentials were averaged over the *xy* plane (along *z* direction). The potentials as a function of position *z* are illustrated in Fig. 4 for Ag interstitials at T_C site with $q = +4e$. The static dielectric constant is 6.52 [53]. The length of the cell is 13.086 Å. The defect-induced potential is well reproduced by the long-range model. The presence of the plateau evidences that the model has correctly reproduced the long-range tail of the defect potential. The charge is well located on the Ag site.

3.4. Diffusion energy barrier

It is generally believed that the diffusion of Ag in 3C-SiC crystalline is the Fickian diffusion[54,11,28]. For the convenience of comparison between various diffusion mechanisms, most studies report the data in form of two-parameter Arrhenius equations. The defect migration and diffusion in general obeys the Arrhenius behaviors, described by the two-parameter Arrhenius equation as $D = D_0\exp(-\frac{E_a}{k_B T})$, where E_a is the activation energy, D_0 is a temperature independent pre-factor, k_B is the Boltzmann constant, T is the temperature. The latest review and comparison of the various diffusion mechanisms with the corresponding D_0 and E_a can be found in Ref. [11,55].

We report our results of the diffusion energy barrier, defined by the activation energy E_a, as a function of the charge state of interstitial Ag in 3C-SiC in line with the literature. As displayed in Fig. 5, the charge state influences the diffusion energy barrier E_a. For the ground state that is neutral, the activation energy is $E_a^m = 1.09$ eV. The maximum of the activation energy $E_a^m = 1.11$ eV is located at $q = +1e$, which is the most common oxidation charge state of Ag ions, as the out most valence electrons are $4d^{10}5s^1$. Whenfro one electron is removed m one Ag atom, the out-most electrons are $4d^{10}$, a full-filled shell, which is a stable charge state. Any further charged states will make the inner electronic shell unfilled, thus decrease the activation energy. For $q = +4e$, the activation energy is 0.894 eV, which is 0.213 eV or 19.2% decrease. Our computed activation energies at various charge states have compared with experiments [28,56] and previous first-principles calculations [24] (Fig. 5).

The activation energies of 1.09 eV ($q = 0$) and 1.11 eV ($q = +1e$) are close to the experimental measurements reported in the literature [56,28]. The activation energy is 1.3 eV (125.3 kJ/mol) from integral release experiments (annealing of irradiated TRISO fuel) [28], and 1.13 from fractional Ag release during irradiation of TRISO fuel [56]. It is worth noting that these experiments [56]. are the best estimate of the

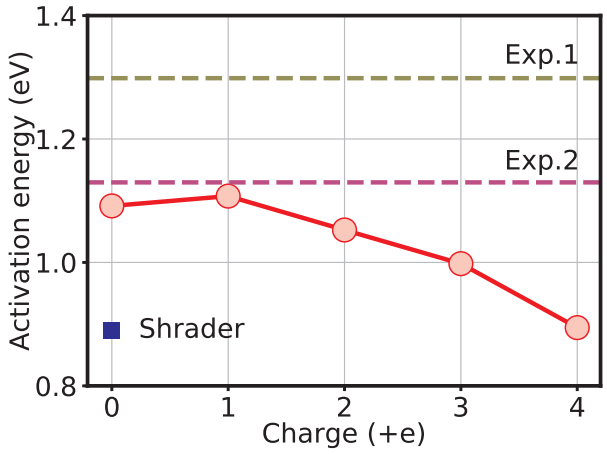

Fig. 5. Activation energy. The activation energy of the bulk Ag diffusion via interstitial as a function of the charge state ranged from 0 to +4e, compared with experiment 1 (1.3 eV, denoted "Expt.1", orange dashed line) [28], experiment 2 (1.13 eV, denoted as "Expt.2", pink dashed line) [56], and the previous DFT study (denoted as "Shrader", blue square) [24].

Ag diffusion under the operation condition in TRISO fuel during the German HTR (high-temperature reactor) fuel program [56]. The coincidence of our migration energy barrier of the interstitial Ag with the "on-site" experiments suggests a scenario of the fast release of Ag through interstitial lattice diffusion.

Such a stringent precondition for mobile Ag could be fulfilled inside a high-temperature reactor in the working condition with high temperature high dose irradiation. Once Ag ions are deposited to interstitials, they will highly likely perform lattice diffusion across the 3C-SiC. The most possible diffusion path is a zigzag pathway along the T_C-T_{Si}-T_C as depicted in Fig. 1. Our results could ring the bell that the lattice diffusion of Ag in 3C-SiC might still play a key role in the Ag release in TRISO fuel under operation conditions.

Recent experiment evidenced the Ag diffusion was greatly enhanced by carbon irradiation [34]. They concluded that the diffusion mechanism is radiation enhanced diffusion via both lattice diffusion and grain boundary diffusion mechanisms. Considering that the experiments are "off-site" with less dose and lower temperature, the experimental results well support our hypothesis that the fast release of Ag through lattice diffusion in 3C-SiC layers in "on-site" TRISO particles.

One precondition for Ag release via lattice diffusion is the large number of Ag in the interstitial sites in 3C-SiC. The solubility of Ag in 3C-SiC is low. It is well known that the formation energy of an interstitial Ag in 3C-SiC is higher than other kinds of defects including the substitutional ones of Ag [37,24]. Therefore, the probability to form substutional Ag defects is higher than forming interstitials. In the mean time, the irradiation generates large number of defects that trap Ag atoms in addition to grain boundaries. As a result, the Ag interstitials could lack long-range diffusion.

Such a difficulty could be overcome by "kickout" reactions proposed by Leng et al. [34]. The black spot defects which are speculated to be the self-interstitial clusters can be dissolved into interstitials [57] at a typical integral release experiment annealing temperature of > 1200 °C, providing a source of self-interstitials. It is evidenced that these black spot defects can provide a significant interstitial source during post-irradiation annealing to potentially enable kicking out every dissolved Ag many times over. These self-interstitials (I) then react with the trapped Ag atoms to kickout Ag atoms back into interstitials. The formation energy of substituted Ag is 7.03 eV and 7.23 eV for Ag_{Si} and Ag_C, respectively [37]. The formation energy of interstitial Ag is 9.89 eV and 10.92 eV for Ag_{T_C} and $Ag_{T_{Si}}$, respectively. The kickout reaction is most likely as $Ag_S + I -> Ag_{T_C}$, where Ag_S is the substitutional Ag and the Ag_{T_C} is the interstitial Ag on the tetrahedra site formed by four carbon atoms. The kickout energy barrier is 2.86 and 2.66 eV for Ag_{Si} and Ag_C, respectively. Such a formation of interstitial Ag_{T_C} by kickout of an isolated substitutional Ag_S is overall energetically favorable among a number of reaction paths [34].

This kickout mechanism seems to be the main cause of the unprecedented Ag release under irradiation, a notorious difficulty hindering the implementation of TRISO. The irradiation provides the required energy to kick-out the substitutional Ag to initiate on jump of bulk diffusion via fast interstitial migration. The kick-out energy with a minimum value of 2.66 eV is otherwise hard to obtain from thermodynamics of the system. The kick-out action could be proceeded by direct head-on collisions with energetic particles or influenced by the irradiation induced shockwaves [58]. In addition, the difference between the experimental activation energies (1.15–1.30 eV) and our theoretical value of 1.09 eV could be used to estimate the kickout rate as an effective factor on top of the activation energy.

A recent theoretical work proposed that a rate-limiting transition state can have a different charge state from the initial ground state, which could significantly lower the activation barrier of a dynamical process that depends on charge state [59]. Here we examine the possible transition state redox during the Ag diffusion in 3C-SiC via lattice diffusion. Using the initial neutral Ag interstitial at T_C site (Ag_{TC}) as the reference state, the energy of both charged states and neutral states are illustrated in Fig. 6.

The minimum energy pathways of the interstitial Ag diffusion with 5 different charge states ranged from neutral to q = +4e using FNV scheme. Although the redox reduces the activation energy of Ag_{TC} during diffusion as illustrated in Fig. 3 and Table 1, the oxidation energies, which is equal to reduction energy, increase much more than the reduced activation energy. The oxidation energies are 0.23, 0.78, 1.65, and 2.85 eV for charge state of $q = 1, 2, 3, 4 + e$, respectively. There is no cross of all these curves Fig. 6. Our results suggest that the transition state redox is unlikely because of the high oxidation energies of Ag. The diffusion process prefer to occur at neutral state without change of the charge status in any transition state.

4. Conclusions

In summary, we revisit the Ag lattice diffusion in a single crystalline 3C-SiC. We investigate the interstitial Ag diffusion via a zigzag pathway along the T_C-T_{Si}-T_C paths by means of first-principles calculations within the framework of density functional theory. The influence of the charge state on the migration energy barriers are explicitly examined. We found that the migration energy barrier of the neutral Ag interstitial diffusion is 1.09 eV, which is 0.2 eV higher than the previous DFT

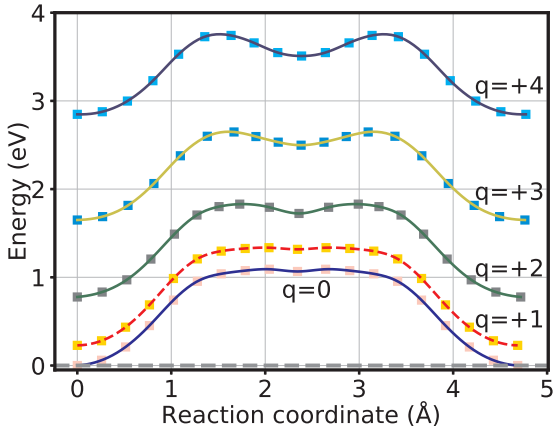

Fig. 6. Redox. Possible transition state redox during dynamical process in the lattice diffusion of the interstitial Ag in 3C-SiC. The reference energy is that of neutral Ag interstitial at T_C site.

calculations. Our more accurate results of spin-polarized DFT calculations in a large simulation cells with 217 atoms with FNV correction set a rigorous ground and reference for further investigation of the other diffusion mechanisms of Ag release in TRISO fuel.

The $+1e$ charged Ag interstitials has a migration energy barrier of 1.11 eV. The activation energy of neutral and $+1e$ charged Ag_{TC} agrees with the activation energy of Ag diffusion measured in the German HTR fuel program [56]. Over charged ($> +1e$) Ag ions possess deeper and wider potential wells in the potential profile along the minimum potential pathways of interstitial diffusion. The migration energy barrier reduces with respect to the charge status of Ag in 3C-SiC. The high oxidation energy suggests that the charge state remains fixed to that of the initial electronic ground state throughout the diffusion. The CI-NEB result suggests that once Ag ions occupy interstitials, the 3C-SiC lattice provides efficient pathways of the T_C-T_{Si}-T_C along the $\langle 1\,0\,1\rangle$ directions for lattice diffusion across the single crystal of 3C-SiC, resulting in fast discharge of Ag in TRISO fuel. Although the Ag could be trapped by defects including vacancies and grain boundaries, the 'kickout' mechanism induced by the irradiation could provide sufficient interstitials supporting long-range lattice diffusion of Ag in 3C-SiC. This finding might reset a solid ground and reference of lattice diffusion for uncovering the silver release in TRISO fuel for secure nuclear energy.

Data availability

The datasets generated during and/or analyzed during the current study are available from the corresponding author on reasonable request.

CRediT authorship contribution statement

Qing Peng: Investigation, Formal analysis, Writing - original draft, Writing - review & editing. **Nanjun Chen:** Investigation, Writing - review & editing. **Zhijie Jiao:** Conceptualization, Writing - review & editing. **Isabella J. van Rooyen:** Conceptualization, Writing - review & editing. **William F. Skerjanc:** Writing - review & editing. **Fei Gao:** Conceptualization, Supervision, Writing - review & editing.

Declaration of Competing Interest

The authors declare that they have no known competing financial interests or personal relationships that could have appeared to influence the work reported in this paper.

Acknowledgement

We thank Dr. Gary Was for useful discussion. The authors would like to acknowledge the generous financial support from Nuclear Energy University Program (NEUP) program.

Appendix A. Supplementary data

Supplementary data associated with this article can be found, in the online version, athttps://doi.org/10.1016/j.commatsci.2019.109190.

References

[1] H. Morkoç, S. Strite, G.B. Gao, M.E. Lin, B. Sverdlov, M. Burns, Large-band-gap SiC, III-V nitride, and II-VI ZnSe-based semiconductor device technologies, J. Appl. Phys. 76 (3) (1994) 1363–1398.
[2] Kim S. Siow, Are sintered silver joints ready for use as interconnect material in microelectronic packaging? J. Electron. Mater. 43 (4) (2014) 947–961.
[3] D. Olander, Nuclear fuels – present and future, J. Nucl. Mater. 389 (1) (2009) 1–22.
[4] E. L'opez-Honorato, J. Tan, P.J. Meadows, G. Marsh, P. Xiao, Triso coated fuel particles with enhanced sic properties, J. Nucl. Mater. 392 (2) (2009) 219–224 Nuclear Fuels and Structural Materials 2.
[5] K. Minato, K. Sawa, T. Koya, T. Tomita, A. Ishikawa, C.A. Baldwin, W.A. Gabbard, C.M. Malone, Fission product release behavior of individual coated fuel particles for high-temperature gas-cooled reactors, Nucl. Technol. 131 (1) (2000) 36–47.
[6] H. Nabielek, P.E. Brown, P. Offermann, Silver release from coated particle fuel, Nucl. Technol. 35 (2) (1977) 483–493.
[7] R.E. Bullock, Fission-product release during post irradiation annealing of several types of coated fuel-particles, J. Nucl. Mater. 125 (3) (1984) 304–319.
[8] K. Minato, T. Ogawa, K. Fukuda, H. Sekino, H. Miyanishi, S. Kado, I. Takahashi, Release behavior of metallic fission-products from HTGR fuel-particles at 1600-degrees to 1900-degrees-C, J. Nucl. Mater. 202 (1–2) (1993) 47–53.
[9] Kazuo Minato, Kazuhiro Sawa, Toshio Koya, Takeshi Tomita, Akiyoshi Ishikawa, Charles A. Baldwin, William Alexander Gabbard, Charlie M. Malone, Fission product release behavior of individual coated fuel particles for high-temperature gas-cooled reactors, Nucl. Technol. 131 (1) (2000) 36–47.
[10] H.J. MacLean, R.G. Ballinger, L.E. Kolaya, S.A. Simonson, N. Lewis, M.E. Hanson, The effect of annealing at 1500 degrees C on migration and release of ion implanted silver in CVD silicon carbide, J. Nucl. Mater. 357 (1–3) (2006) 31–47.
[11] Hyunseok Ko, Jie Deng, Izabela Szlufarska, Dane Morgan, Ag diffusion in sic high-energy grain boundaries: kinetic monte carlo study with first-principle calculations, Comput. Mater. Sci. 121 (2016) 248–257.
[12] W. Schenk, G. Pott, H. Nabielek, Fuel accident performance testing for small htrs, J. Nucl. Mater. 171 (1) (1990) 19–30.
[13] E. Friedland, J.B. Malherbe, N.G. van der Berg, T. Hlatshwayo, A.J. Botha, E. Wendler, W. Wesch, Study of silver diffusion in silicon carbide, J. Nucl. Mater. 389 (2) (2009) 326–331.
[14] H.Y. Xiao, Y. Zhang, L.L. Snead, V. Shutthanandan, H.Z. Xue, W.J. Weber, Near-surface and bulk behavior of ag in sic, J. Nucl. Mater. 420 (1) (2012) 123–130.
[15] Eddie Lopez-Honorato, DaXiang Yang, Jun Tan, Philippa J. Meadows, Ping Xiao, Silver diffusion in coated fuel particles, J. Am. Ceram. Soc. 93 (10) (2010) 3076–3079.
[16] Ying Chen, Christopher A. Schuh, Diffusion on grain boundary networks: percolation theory and effective medium approximations, Acta Mater. 54 (18) (2006) 4709–4720.
[17] D.A. Petti, J. Buongiorno, J.T. Maki, R.R. Hobbins, G.K. Miller, Key differences in the fabrication, irradiation and High Temp. Accident testing of US and German TRISO-coated particle fuel, and their implications on fuel performance, Nucl. Eng. Des. 222 (2–3) (2003) 281–297.
[18] E. Friedland, N.G. van der Berg, J.B. Matherbe, J.J. Hancke, J. Barry, E. Wendler, W. Wesch, Investigation of silver and iodine transport through silicon carbide layers prepared for nuclear fuel element cladding, J. Nucl. Mater. 410 (1–3) (2011) 24–31.
[19] Eddie Lopez-Honorato, Huixing Zhang, DaXiang Yang, Ping Xiao, Silver diffusion in silicon carbide coatings, J. Am. Ceram. Soc. 94 (9) (2011) 3064–3071.
[20] I.J. van Rooyen, T.M. Lillo, Y.Q. Wu, Identification of silver and palladium in irradiated TRISO coated particles of the AGR-1 experiment, J. Nucl. Mater. 446 (1–3) (2014) 178–186.
[21] R.J. Lauf, T.B. Lindemer, R.L. Pearson, Out-of-reactor studies of fission product-silicon carbide interactions in htgr fuel particles, J. Nucl. Mater. 120 (1) (1984) 6–30.
[22] J.H. Neethling, J.H. O'Connell, E.J. Olivier, Palladium assisted silver transport in polycrystalline sic, Nucl. Eng. Des. 251 (2012) 230–234 5th International Topical Meeting on High Temp. ReactOR Technology (HTR 2010).
[23] Xin Geng, Fan Yang, Nadia Rohbeck, Ping Xiao, An original way to investigate silver migration through silicon carbide coating in TRISO particles, J. Am. Ceram. Soc. 97 (6) (2014) 1979–1986.
[24] David Shrader, Sarah M. Khalil, Tyler Gerczak, Todd R. Allen, Andrew J. Heim, Izabela Szlufarska, Dane Morgan, Ag diffusion in cubic silicon carbide, J. Nucl. Mater. 408 (3) (2011) 257–271.
[25] Sarah Khalil, Narasimhan Swaminathan, David Shrader, Andrew J. Heim, Dane D. Morgan, Izabela Szlufarska, Diffusion of Ag along Sigma 3 grain boundaries in 3C-SiC, Phys. Rev. B 84 (21) (2011) 214104.
[26] Jeremy Rabone, Eddie Lopez-Honorato, Paul Van Uffelent, Silver and cesium diffusion dynamics at the beta-SiC Sigma 5 grain boundary investigated with density functional theory molecular dynamics and metadynamics, J. Phys. Chem. A 118 (5) (2014) 915–926.
[27] Jie Deng, Hyunseok Ko, Paul Demkowicz, Dane Morgan, Izabela Szlufarska, Grain boundary diffusion of Ag through polycrystalline SiC in TRISO fuel particles, J. Nucl. Mater. 467 (1) (2015) 332–340.
[28] Bong Goo Kim, Sunghwan Yeo, Young Woo Lee, Moon Sung Cho, Comparison of diffusion coefficients and activation energies for ag diffusion in silicon carbide, Nucl. Eng. Technol. 47 (5) (2015) 608–616.
[29] T.M. Lillo, I.J. van Rooyen, J.A. Aguiar, Silicon carbide grain boundary distributions, irradiation conditions, and silver retention in irradiated AGR-1 TRISO fuel particles, Nucl. Eng. Des. 329 (2018) 46–52.
[30] Haiming Wen, Isabella J. van Rooyen, Distribution of fission products palladium, silver, cerium and cesium in the un-corroded areas of the locally corroded sic layer of a neutron irradiated triso fuel particle, J. Eur. Ceram. Soc. 37 (10) (2017) 3271–3284.
[31] B. Leng, I.J. van Rooyen, Y.Q. Wu, I. Szlufarska, K. Sridharan, Stem-eds analysis of fission products in neutron-irradiated triso fuel particles from agr-1 experiment, J. Nucl. Mater. 475 (2016) 62–70.
[32] I.J. van Rooyen, E.J. Olivier, J.H. Neethling, Fission products silver, palladium, and cadmium identification in neutron-irradiated sic triso particles using a cs-corrected hrtem, J. Nucl. Mater. 476 (2016) 93–101.
[33] Tyler J. Gerczak, Bin Leng, Kumar Sridharan, Jerry L. Hunter, Andrew J. Giordani, Todd R. Allen, Observations of ag diffusion in ion implanted sic, J. Nucl. Mater. 461 (2015) 314–324.
[34] Bin Leng, Hyunseok Ko, Tyler J. Gerczak, Jie Deng, Andrew J. Giordani, Jerry L. Hunter, Dane Morgan, Izabela Szlufarska, Kumar Sridharan, Effect of carbon ion

irradiation on Ag diffusion in SiC, J. Nucl. Mater. 471 (2016) 220–232.
[35] Isabella Van Rooyen, Thomas Lillo, Haiming Wen, Connie Hill, Terry Holesinger, Yaqiao Wu, Jeffery Aguiar, Micro/nano-structural examination and fission product identification in neutron irradiated Agr-1 TRISO Fuel, International Topical Meeting on High Temp, ReactOR Technology, HTR, 2016.
[36] Ying Chen, Christopher A. Schuh, Geometric considerations for diffusion in polycrystalline solids, J. Appl. Phys. 101 (6) (2007) 063524.
[37] Nanjun Chen, Qing Peng, Zhijie Jiao, Isabella van Rooyen, William F. Skerjanc, Fei Gao, Ab initio study of the stability of intrinsic and extrinsic ag point defects in 3csic, J. Nucl. Mater. 510 (2018) 596–602.
[38] G. Kresse, J. Hafner, Ab initio molecular dynamics for liquid metals, Phys. Rev. B 47 (1993) 558.
[39] G. Kresse, J. Furthuller, Efficiency of ab-initio total energy calculations for metals and semiconductors using a plane-wave basis set, Comput. Mater. Sci. 6 (1996) 15.
[40] P. Hohenberg, W. Kohn, Inhomogeneous electron gas, Phys. Rev. 136 (3B) (1964) B864.
[41] W. Kohn, L.J. Sham, Self-consistent equations including exchange and correlation effects, Phys. Rev. 140 (4A) (1965) A1133.
[42] John P. Perdew, Kieron Burke, Matthias Ernzerhof, Generalized gradient approximation made simple, Phys. Rev. Lett. 77 (1996) 3865–3868.
[43] John P. Perdew, Adrienn Ruzsinszky, Gábor I. Csonka, Oleg A. Vydrov, Gustavo E. Scuseria, Lucian A. Constantin, Xiaolan Zhou, Kieron Burke, Restoring the density-gradient expansion for exchange in solids and surfaces, Phys. Rev. Lett. 100 (2008) 136406.
[44] P.E. Blöchl, Projector augmented-wave method, Phys. Rev. B 50 (24) (1994) 17953–17979.
[45] R.O. Jones, O. Gunnarsson, The density functional formalism, its applications and prospects, Rev. Mod. Phys. 61 (3) (Jul 1989) 689–746.
[46] Christoph Freysoldt, Jörg Neugebauer, Chris G. Van de Walle, Fully ab initio finite-size corrections for charged-defect supercell calculations, Phys. Rev. Lett. 102 (2009) 016402.
[47] Christoph Freysoldt, Blazej Grabowski, Tilmann Hickel, Jörg Neugebauer, Georg Kresse, Anderson Janotti, Chris G. Van de Walle, First-principles calculations for point defects in solids, Rev. Mod. Phys. 86 (2014) 253–305.
[48] Graeme Henkelman, Blas P. Uberuaga, Hannes Jónsson, A climbing image nudged elastic band method for finding saddle points and minimum energy paths, J. Chem. Phys. 113 (22) (2000) 9901–9904.
[49] O. Madelung, U. Rössler, M. Schulz (Eds.), Silicon Carbide (SiC), Lattice Parameters, Thermal Expansion, Springer Berlin Heidelberg, Berlin, Heidelberg, 2002, pp. 1–11.
[50] Ruixuan Han, Liucheng Liu, Rui Tu, Wei Xiao, Yingying Li, Huailin Li, Dan Shao, Iodine atom diffusion in SiC and zirconium with first-principles calculations, Nucl. Technol. 195 (2) (2016) 192–203.
[51] Stefan Grimme, Jens Antony, Stephan Ehrlich, Helge Krieg, A consistent and accurate ab initio parametrization of density functional dispersion correction (DFT-D) for the 94 elements H-Pu, J. Chem. Phys. 132 (15) (2010) 154104.
[52] Qing Peng, Guangyu Wang, Gui-Rong Liu, Suvranu De, Van der waals density functional theory vdw-dfq for semihard materials, Crystals 9 (5) (2019) 243.
[53] George Theodorou, George Tsegas, Efthimios Kaxiras, Theory of electronic and optical properties of 3c-sic, J. Appl. Phys. 85 (4) (1999) 2179–2184.
[54] Tyler J. Gerczak, Bin Leng, Kumar Sridharan, Jerry L. Hunter, Andrew J. Giordani, Todd R. Allen, Observations of Ag diffusion in ion implanted SiC, J. Nucl. Mater. 461 (2015) 314–324.
[55] Johan B. Malherbe, Diffusion of fission products and radiation damage in sic, J. Phys. D: Appl. Phys. 46 (47) (2013) 473001.
[56] J.J. van der Merwe, Evaluation of silver transport through SiC during the German HTR fuel program, J. Nucl. Mater. 395 (1–3) (2009) 99–111.
[57] Yoshiyuki Watanabe, Kazunori Morishita, Yasunori Yamamoto, Nucleation and growth of self-interstitial atom clusters in -sic during irradiation: kinetic monte-carlo modeling, Nucl. Instrum. Methods Phys. Res. Sect. B 269 (14) (2011) 1698–1701 Computer Simulations of Radiation Effects in Solids.
[58] Qing Peng, Fanjiang Meng, Yizhong Yang, Lu. Chenyang, Huiqiu Deng, Luming Wang, Suvranu De, Fei Gao, Shockwave generates < 100 > dislocation loops in bcc iron, Nat. Commun. 9 (2018) 4880.
[59] Guangfu Luo, Thomas F. Kuech, Dane Morgan, Transition state redox during dynamical processes in semiconductors and insulators, NPG Asia Mater. 10 (2018) 45–51.